

Multicriticality of the three-dimensional Ising model with plaquette interactions: An extension of Novotny's transfer-matrix formalism

Yoshihiro Nishiyama

Department of Physics, Faculty of Science, Okayama University, Okayama 700-8530, Japan

(Received 11 April 2004; published 31 August 2004)

A three-dimensional Ising model with the plaquette-type (next-nearest-neighbor and four-spin) interactions is investigated numerically. This extended Ising model, the so-called gonihedric model, was introduced by Savvidy and Wegner as a discretized version of the interacting (closed) surfaces without surface tension. The gonihedric model is notorious for its slow relaxation to the thermal equilibrium (glassy behavior), which deteriorates the efficiency of the Monte Carlo sampling. We employ the transfer-matrix (TM) method, implementing Novotny's idea, which enables us to treat an arbitrary number of spins N for one TM slice even in three dimensions. This arbitrariness admits systematic finite-size-scaling analyses. Accepting the extended parameter space by Cirillo *et al.*, we analyzed the (multi-) criticality of the gonihedric model for $N \leq 13$. Thereby, we found that, as first noted by Cirillo *et al.* analytically (cluster-variation method), the data are well described by the multicritical (crossover) scaling theory. That is, the previously reported nonstandard criticality for the gonihedric model is reconciled with a crossover exponent and the ordinary three-dimensional-Ising universality class. We estimate the crossover exponent and the correlation-length critical exponent at the multicritical point as $\phi=0.6(2)$ and $\nu=0.45(15)$, respectively.

DOI: 10.1103/PhysRevE.70.026120

PACS number(s): 05.70.Np, 64.60.-i, 05.10.-a, 05.50.+q

I. INTRODUCTION

Study on surfaces spans a wide variety of subjects ranging from biochemistry to high-energy physics [1,2], leading to a very active area of research. In particular, the problem of interacting surface gas [3–6] is of fundamental significance. The Savvidy-Wegner (gonihedric) model [7–11] describes the interacting closed surfaces without surface tension. The surfaces are discretized in such a way that they are embedded in the three-dimensional cubic lattice, and the surface faces consist of plaquettes. The gonihedric model was introduced as a lattice-regularized version of the string field theory [12]. However, recent developments dwell on the case of three dimensions, aiming a potential applicability to microemulsions.

The gonihedric model admits a familiar representation in terms of the Ising-spin variables $\{S_i\}$ through the duality transformation; namely, the plaquette surfaces are regarded as the magnetic-domain interfaces. To be specific, the Hamiltonian is given by the following form:

$$H = J_1 \sum_{\langle i,j \rangle} S_i S_j + J_2 \sum_{\langle\langle i,j \rangle\rangle} S_i S_j + J_3 \sum_{[i,j,k,l]} S_i S_j S_k S_l, \quad (1)$$

with finely tuned coupling constants, $J_1 = -2\kappa$, $J_2 = \kappa/2$, and $J_3 = -(1-\kappa)/2$. The Ising spins $S_i = \pm 1$ are placed at the cubic-lattice points in three dimensions, and the summations $\sum_{\langle i,j \rangle}$, $\sum_{\langle\langle i,j \rangle\rangle}$, and $\sum_{[i,j,k,l]}$ run over all possible nearest-neighbor pairs, next-nearest-neighbor (plaquette diagonal) spins, and round-a-plaquette spins, respectively. The interfacial energy E of the gonihedric model is given by the formula $E = n_2 + 4\kappa n_4$, where n_2 is the number of links where two plaquettes meet at a right angle (folded-link length) and n_4 is the number of links where four plaquettes meet at right angles (self-intersection-link length). Namely, the surfaces are subjected to a bending elasticity with a fixed strength,

and the self-avoidance is controlled by the parameter κ . We notice that the interfacial energy lacks the surface-tension term.

Because of the absence of the surface tension, thermally activated undulations should be promoted significantly. Such a feature might be reflected by the phase diagram; see Fig. 1(a) [13,14]. We notice that a phase transition occurs at a considerably low temperature quite reminiscent of that of the two-dimensional Ising model. Moreover, for large κ , the phase transition becomes a continuous one, whose criticality has been arousing much attention: By means of the Monte Carlo method, Johnston and Malmi [15] obtained the critical exponents $\nu=1.2(1)$, $\gamma=1.60(2)$, and $\beta=0.12(1)$ for the self-avoidance $\kappa=1$. (Here, we quoted one typical set of exponents among those reported in the literature by various

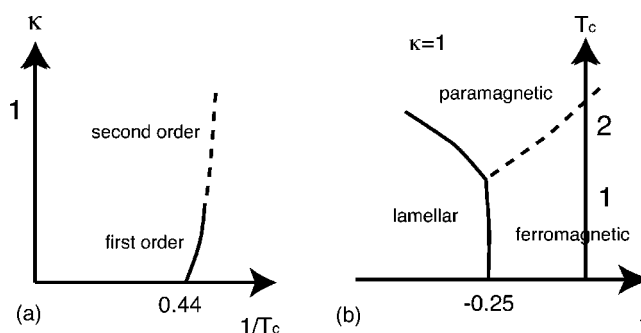


FIG. 1. (a) A schematic phase diagram for the gonihedric model (1) is shown [13]. For large κ , second-order phase transition occurs. The criticality has been arousing much attention. (b) For an extended parameter space, Eq. (2), there emerge rich phases accompanying a multicritical point [22]; here, the self-avoidance parameter κ is fixed ($\kappa=1$). In terms of this extended parameter space, the transition point in (a) is identified with the multicritical point at $j = -0.25$.

means.) The authors claimed that the exponents bear remembrance to those of the two-dimensional Ising model, namely, $\nu=1$, $\gamma=7/4$, and $\beta=1/8$. On the other hand, with the Monte Carlo method, Baig *et al.* [16] obtained $\nu=0.44(2)$ ($\kappa=1$) and $\gamma/\nu=2.1(1)$ ($\kappa=0.5, 1$). By means of the low-temperature series expansion, Pietig and Wegner [17] obtained $\alpha=0.62(3)$, $\beta=0.040(2)$, and $\gamma=1.7(2)$ ($\kappa=1$). With the use of the cluster-variation method with the aid of the Padé approximation [18–21], Cirillo *et al.* obtained the estimates $\beta=0.062(3)$ and $\gamma=1.41(2)$.

Meanwhile, a subtlety of the Monte Carlo simulation inherent to the gonihedric model was noted by Hellmann *et al.* [22]. According to them, the relaxation to the thermal equilibrium is extremely slow, and such slow relaxation smears out the singularity of the phase transition. In order to cope with such slow relaxation (long autocorrelation length), they employed the histogram Monte Carlo method. However, the singularity of the phase transition could not be resolved satisfactorily. (See also Ref. [20] for an alternative evidence of strong metastabilities.) As a matter of fact, the gonihedric model at $\kappa=0$ reduces to the so-called ferromagnetic p -spin model, and the model has been studied extensively as a possible lattice realization of supercooled liquids and glassy behaviors [23–28]. In this sense, an alternative simulation scheme other than the Monte Carlo method is desirable in order to surmount the slow-relaxation problem and determine the critical exponents reliably.

In this paper, we develop a transfer-matrix formalism, implementing Novotny's idea [31–34], which enables us to treat an arbitrary number of spins N for one transfer-matrix slice. This arbitrariness admits systematic finite-size-scaling analyses. (In addition to this advantage, the transfer-matrix calculation yields the correlation length ξ directly. Because ξ has a fixed scaling dimension, succeeding effort at the finite-size-scaling analyses is reduced to a considerable extent.) We also accept the idea of Cirillo *et al.* [19], who extended the parameter space of the gonihedric model (1) to

$$J_1 = -1, \quad J_2 = -j, \quad \text{and} \quad J_3 = -\frac{1-\kappa}{4\kappa}. \quad (2)$$

(Note that for $j=-0.25$, the parameter space reduces to that of the aforementioned original gonihedric model.) With respect to this extended parameter space, Cirillo *et al.* claimed that the above-mentioned peculiar criticality could be identified with a mere end-point singularity (multicriticality) [29,30] of an ordinary critical line of the three-dimensional-Ising universality class; see the critical branch of the phase diagram shown in Fig. 1(b). Thereby, they obtained the crossover critical exponent $\phi=1.1(1)$ by means of the cluster-variation method [19]. Our transfer-matrix simulation supports their idea that the numerical data are well described by the multicritical (crossover) scaling theory. We estimate the crossover exponent and the correlation-length critical exponent as $\phi=0.6(2)$ and $\nu=0.45(15)$, respectively; hereafter, we place a dot over the critical indices at the multicritical point ($j=-0.25$).

The rest of this paper is organized as follows. In Sec. II we set up a transfer-matrix formalism for the gonihedric

model based on Novotny's idea. In Sec. III we present the numerical results. Taking advantage of the Novotny formalism, we carry out systematic finite-size-scaling analyses. In the last section, we present summary and discussions.

II. EXTENSION OF THE NOVOTNY METHOD TO THE PLAQUETTE-TYPE INTERACTIONS

In this section, we present methodological details of our numerical simulation for the gonihedric model (1). We employed Novotny's improved version [31–33] of the transfer-matrix method. This technique allows us to construct the transfer matrices containing an arbitrary number of spins N in one transfer-matrix slice; note that in the conventional scheme, the available system sizes N are limited for high spatial dimensions $d \geq 3$ severely. Actually, Novotny constructed the transfer matrices of the Ising model for $d \leq 7$ fairly systematically [34]. Such arbitrariness of N admits systematic finite-size-scaling analyses.

In the following, we adopt Novotny's idea to study the gonihedric model (1). For that purpose, we extend his idea so as to incorporate plaquette-based interactions. We restrict ourselves to the case of three dimensions $d=3$ relevant to our concern. (The original idea of Novotny is formulated systematically for general dimensions, taking the advantage that only the bond-based (nearest neighbor) interaction is involved.)

We decompose the transfer matrix into the following three components:

$$T = T^{(\text{leg})} \odot T^{(\text{planar})} \odot T^{(\text{rung})}, \quad (3)$$

where the symbol \odot denotes the Hadamard (element by element) matrix multiplication. Note that the multiplication of the local Boltzmann weights should give rise to the total Boltzmann factor. The decomposed parts, $T^{(\text{leg})}$, $T^{(\text{planar})}$, and $T^{(\text{rung})}$, of Eq. (3) stand for the Boltzmann weights for intraleg plaquettes, intraplanar plaquettes, and rung plaquettes, respectively; see Fig. 2 as well.

First, let us consider the contribution of $T^{(\text{leg})}$. The matrix elements are given by the formula

$$T_{ij}^{(\text{leg})} = \langle i|A|j \rangle = W_{S(i,1)S(i,2)}^{S(i,1)S(j,2)} W_{S(i,2)S(i,3)}^{S(i,2)S(j,3)} \cdots W_{S(i,N)S(i,1)}^{S(j,N)S(j,1)}, \quad (4)$$

where the indices i and j specify the spin configurations for both sides of the transfer-matrix slice. More specifically, we consider N spins for a transfer-matrix slice, and the index i specifies a spin configuration $\{S(i,1), S(i,2), \dots, S(i,N)\}$ arranged along the leg; see Fig. 2. The factor $W_{S_1 S_2}^{S_3 S_4}$ denotes the local Boltzmann weight for a plaquette with corner spins $\{S_1, \dots, S_4\}$. Explicitly, it is given by the following form:

$$W_{S_1 S_2}^{S_3 S_4} = \exp \left[-\frac{1}{T} \left(\frac{J_1}{4} (S_1 S_2 + S_2 S_4 + S_4 S_3 + S_3 S_1) + \frac{J_2}{2} (S_1 S_4 + S_2 S_3) + \frac{J_3}{2} S_1 S_2 S_3 S_4 \right) \right]. \quad (5)$$

(The denominators of the coupling constants are intended to avoid double counting.) Here, the parameter T denotes the temperature. It is to be noted that the component $T^{(\text{leg})}$, with

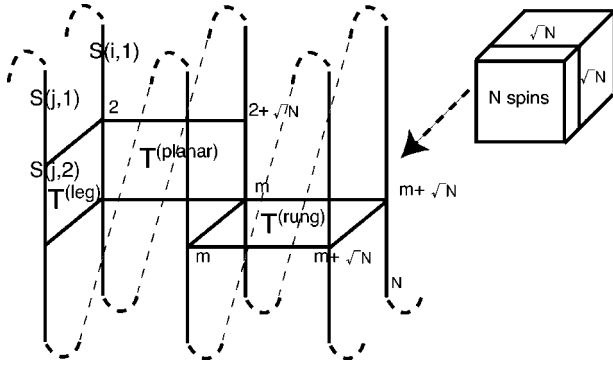


FIG. 2. Novotny invented a new scheme to construct the transfer matrix (TM) [31–33], which allows us to treat an arbitrary number of spins N per one TM slice. We extend his scheme to incorporate the plaquette-type (next-nearest-neighbor and four-spin) interactions, aiming to treat the gonihedric model (1). The contributions from the “leg,” “planar,” and “rung” interactions are considered separately; see Eq. (3). With use of the translation operator $P^{\sqrt{N}}$, we build a bridge between the \sqrt{N} th neighbor spins along the leg (interleg interaction).

the other components ignored, leads the transfer-matrix for the two-dimensional gonihedric model. The other components of $T^{(\text{planar})}$ and $T^{(\text{rung})}$ should introduce the “interleg” interactions so as to raise the dimensionality to $d=3$.

Second, we consider the component for the intraplanar interaction. It is constructed by the following formula,

$$T_{ij}^{(\text{planar})} = \langle i | A P^{\sqrt{N}} | i \rangle, \quad (6)$$

where the matrix P denotes the translation operator; namely, with the operation, a spin arrangement $\{S(i, m)\}$ is shifted to $\{S(i, m+1)\}$; the periodic boundary condition is imposed. An explicit representation of P is given afterward. Because of the insertion of $P^{\sqrt{N}}$, the plaquette interaction A bridges the \sqrt{N} th-nearest-neighbor pairs, and so, it brings about the desired interleg interactions. This is an essential idea of Novotny’s work. A crucial point is that the operation $P^{\sqrt{N}}$ is still meaningful, even though the power \sqrt{N} is an irrational number [31–33]. This rather remarkable fact renders freedom that one can choose an arbitrary number of spins.

An explicit representation of P^x is given as follows [31–33]. As is well known, the eigenvalues $\{p_k\}$ of P belong to the N roots of unity like $\exp(i\phi_k)$ with $\phi_k = 2\pi k/N$ ($k=0, 1, \dots, N-1$). The complete set of the corresponding eigenvectors are constructed by the formula $|\Phi_k\rangle = N_{\Phi_k}^{-1} \sum_{l=1}^N p_k^l P^l |\Phi\rangle$. Here, the set $\{|\Phi\rangle\}$ consists of such bases independent with respect to the translation operations, and $N_{\Phi_k}^{-1}$ is a normalization factor. Provided that the eigenstates $|\Phi_k\rangle$ are at hand, one arrives at an explicit representation of P^x ;

$$\langle i | P^x | j \rangle = \sum_{\Phi_k} \langle i | \Phi_k \rangle p_k^x \langle \Phi_k | j \rangle. \quad (7)$$

Finally, we consider the component of $T^{(\text{rung})}$. This component is also constructed similarly. This time, however, we need two operations of $P^{\sqrt{N}}$, because $T^{(\text{rung})}$ concerns both

sectors of i and j (both sides of the transfer-matrix slice); see Fig. 2. The elements are given by

$$T_{ij}^{(\text{rung})} = \langle \langle i | \otimes \langle j | \rangle B[(P^{\sqrt{N}} | i \rangle) \otimes (P^{\sqrt{N}} | j \rangle)], \quad (8)$$

where the operator B acts on the direct-product space;

$$\langle \langle i | \otimes \langle j | \rangle B(|k\rangle \otimes |l\rangle) = \prod_{m=1}^N W_{S(i,m)S(j,m)}^{S(k,m)S(l,m)}. \quad (9)$$

Putting the components $T^{(\text{leg})}$, $T^{(\text{planar})}$, and $T^{(\text{rung})}$ into Eq. (3), we obtain the complete form of the transfer matrix. Actual numerical diagonalizations are performed in the following section.

III. NUMERICAL RESULTS

In this section we survey the criticality of the gonihedric model (1) for the extended parameter space (2) by means of the transfer-matrix method developed in the preceding section. In particular, we investigate the critical branch with an emphasis on the end-point singularity at $j=-0.25$. We neglect a possible deviation of the multicritical point from $j=-0.25$ as pointed out by the cluster-variation-method study [19]. Such deviation is so slight that it would not affect the multicritical analyses very seriously [19]. We treated the system sizes up to $N=13$. The system sizes N are restricted to odd numbers, for which the transfer-matrix elements consist of real numbers [31–33].

A. Survey of the critical branch with the Roomany-Wyld approximative beta function

To begin with, we survey the criticality of the second-order phase boundary in Fig. 1(b). For that purpose, we calculated the Roomany-Wyld approximative beta function $\beta^{RW}(T)$. We stress that the availability of the $\beta^{RW}(T)$ is one of the major advantages of the transfer-matrix method. The Roomany-Wyld beta function is given by the following formula [35]:

$$\beta_N^{RW}(T) = - \frac{1 - \frac{\ln[\xi_N(T)/\xi_{N-2}(T)]}{\ln(\sqrt{N}/\sqrt{N-2})}}{\sqrt{\frac{\partial_T \xi_N(T) \partial_T \xi_{N-2}(T)}{\xi_N(T) \xi_{N-2}(T)}}}. \quad (10)$$

Here, $\xi_N(T)$ denotes the correlation length for the system size N . The correlation length is readily calculated by means of the transfer-matrix method. That is, using the largest and next-largest eigenvalues, namely, λ_1 and λ_2 , of the transfer matrix, we obtain the correlation length $\xi = 1/\ln(\lambda_1/\lambda_2)$ immediately.

In Fig. 3 we plotted the β function $\beta_{13}^{RW}(T)$ for various j with the fixed self-avoidance parameter $\kappa=2$. The zero point (fixed point) of the β function $\beta_{13}^{RW}(T)$ indicates the location of the critical point T_c . In the inset of Fig. 3, we plotted the phase-transition point $T_c(j)$. This phase boundary corresponds to the critical branch of the phase diagram shown in Fig. 1(b); the other phase boundaries are of first order, and

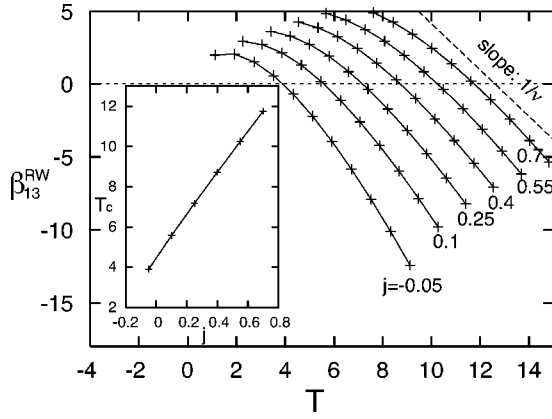


FIG. 3. The β function $\beta_{13}^{RW}(T)$ (10) is plotted for $\kappa=2$ and various j . For a comparison, we presented a slope (dashed line) corresponding to the three-dimensional-Ising universality class ($\nu=0.6294$ [36]); we see that the criticality is maintained to be the three-dimensional-Ising universality class for a wide range of j . In fact, from the slopes at the fixed points of $\beta_{13}^{RW}(T)$, we obtain an estimate for the correlation-length critical exponent $\nu=0.638(5)$; see text for details. Inset: Plotting the zero points of $\beta_{13}^{RW}(T)$, we determine a phase boundary $T_c(j)$, which corresponds to the critical branch in Fig. 1(b).

the determination of them is out of the scope of the present $\beta_N^{RW}(T)$ approach.

The slope of the β function at $T=T_c$ yields an estimate for the inverse of the correlation-length critical exponent $1/\nu$. In Fig. 3 we also presented a slope (dashed line) corresponding to the three-dimensional-Ising universality class $\nu=0.6294$ [36] for a comparison. We see that the criticality is maintained to be the three-dimensional-Ising universality class for a wide range of j . More specifically, for $j=-0.05, 0.1, 0.25, 0.4, 0.55,$ and 0.7 , we obtained the correlation-length critical exponent as $\nu=0.634, 0.641, 0.643, 0.642,$ and 0.642 , respectively. From this observation, we estimated the exponent along the critical branch as $\nu=0.638(5)$ fairly in good agreement with the three-dimensional-Ising universality class.

It is to be noted that, as mentioned in the Introduction, at $j=-0.25$, very peculiar critical exponents have been reported so far [15–17,19]. The above simulation result suggests that such peculiar criticality should be realized only at $j=-0.25$ (critical end point). This idea was first claimed by Ref. [19] with the cluster-variation method. In fact, on closer inspection, the β function in Fig. 3 shows a crossover behavior such that the slope in the off-critical regime is enhanced; see the regime of $T-T_c > 3$ at $j=-0.05$ in particular. It appears that such a regime of enhancement is pronounced as $j \rightarrow -0.25$. Eventually, right at $j=-0.25$, a new universality accompanying small $\nu (< \nu)$ may emerge. In the succeeding sections, we provide further support to this issue.

For the region in close vicinity to the critical end point, for instance, $-0.25 < j < -0.2$, we found that the β function acquires unsystematic finite-size corrections; even the zero point of $\beta_N^{RW}(T)$ disappears. In this sense, we suspect that a direct simulation at $j=-0.25$ would not be very efficient. Rather, performing simulations for a wide range of j , we are

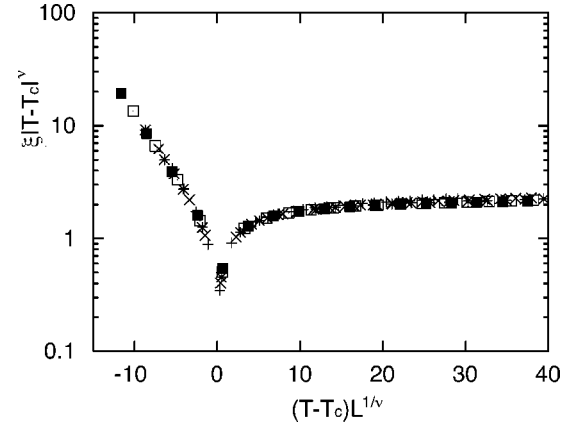


FIG. 4. Scaling plot for the correlation length, namely, $(T-T_c)L^{1/\nu} - \xi|T-T_c|^\nu$, is shown for $\kappa=2$ and $j=0.3$. Here, we postulated the three-dimensional-Ising universality class $\nu=0.6294$ [36]. The symbols $+, \times, *, \square,$ and \blacksquare denote the system sizes of $N=5, 7, 9, 11,$ and 13 , respectively. We confirm that the transition belongs to the three-dimensional-Ising universality class. Furthermore, from the plateau in the high-temperature side, we obtain an estimate for the critical amplitude $N^+=2.09(13)$; see text for details.

able to extract information concerning the end-point singularity fairly reliably.

B. End-point singularity of the critical amplitude of ξ

In the above, we found that the universality class of the critical branch is maintained to be that of the three-dimensional Ising model. A notable feature is that a crossover to a new universality class emerges as $j \rightarrow -0.25$. In this section, we study this multicriticality in terms of the theory of the crossover critical phenomenon. We read off the crossover exponent ϕ from the end-point singularity of the amplitude [30] of the correlation length. Namely, the correlation length should diverge in the form

$$\xi \approx N^\pm |T - T_c|^{-\nu}, \quad (11)$$

with the amplitude

$$N^\pm \propto \Delta^{(-\nu+\nu)/\phi}. \quad (12)$$

Here, the variable Δ denotes the distance from the multicritical point $\Delta=j+0.25$. (It is to be noted that the critical point T_c depends on Δ as demonstrated in the inset of Fig. 3.) The above formula is a straightforward consequence of the multicritical (crossover) scaling hypothesis [29,30];

$$\xi \approx |T - T_c|^{-\nu} X(\Delta/|T - T_c|^\phi). \quad (13)$$

As noted in the previous section, the dotted critical index stands for that right at the multicritical point.

To begin with, we determine the critical amplitude N^+ . In Fig. 4, we plotted the scaled correlation length $(T-T_c)L^{1/\nu} - \xi|T-T_c|^\nu$ for $\kappa=2$ and $j=0.3$. The symbols $+, \times, *, \square,$ and \blacksquare denote the system sizes of $N=5, 7, 9, 11,$ and 13 , respectively. The linear dimension of the system L is given by $L=\sqrt{N}$. In the plot, we postulated the three-dimensional-Ising universality class $\nu=0.6294$ [36]. We see that the scaled data

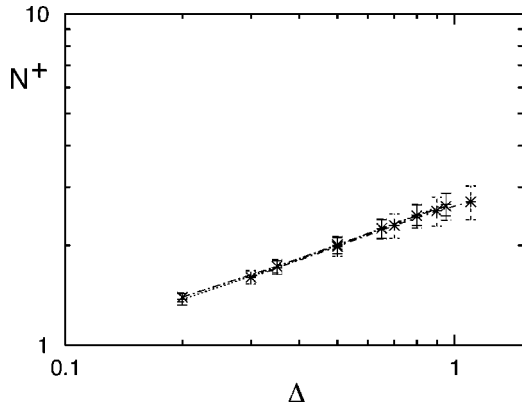


FIG. 5. Correlation-length critical amplitude N^+ (12) is plotted for various $\Delta(=j+0.25)$ and $\kappa=0.5, 1$, and 4 . The symbols $+$, \times , and $*$ stand for the self-avoidance parameter $\kappa=0.5, 1$, and 4 , respectively. The data indicate a clear power-law singularity, Eq. (12). From the slopes, we estimate the singularity exponent as $(-\dot{\nu} + \nu)/\phi=0.415(20)$.

collapse into a scaling-function curve. We again confirm that the phase transition belongs to the three-dimensional-Ising universality class. In addition to this, from the limiting value of the high-temperature side of the scaling function, we estimate the critical amplitude as $N^+=2.09(13)$ for $\kappa=2$ and $j=0.3$; more specifically, we read off the value of $N=13$ around the regime $(T-T_c)L^{1/\nu} \approx 30$, and as for an error indicator, we accepted the amount of the data scatter among $N=5, \dots, 13$.

Similarly, we determined N^+ for various parameter ranges of both j and κ . In Fig. 5, we plotted the amplitude N^+ for $\kappa=1, 2$, and 4 with $\Delta(=j+0.25)$ varied. In the plot, we observe a clear signature of the power-law singularity as described by Eq. (12). Hence we confirm that the cross-over behavior (13) is realized actually around the multicritical point $j=-0.25$. Moreover, in the figure, we notice that the data for $\kappa=1, 2$, and 4 almost overlap each other. It would be rather remarkable that the amplitude N^+ itself hardly depends on the parameter κ . This fact indicates that the multicriticality, namely, the singularity exponent $(-\dot{\nu} + \nu)/\phi$, stays universal with respect to the self-avoidance parameter κ . Such universality was first reported by the series-expansion analyses surveying the range of $\kappa=0.5, \dots, 3$ [17].

From the slopes in Fig. 5 we obtained the singularity exponent as $(-\dot{\nu} + \nu)/\phi=0.422(6)$, $0.405(5)$, and $0.415(7)$ for $\kappa=1, 2$, and 4 , respectively. We estimate the singularity exponent as $(-\dot{\nu} + \nu)/\phi=0.415(20)$ consequently.

Let us mention some remarks on this estimate $(-\dot{\nu} + \nu)/\phi=0.415(20)$. First, this result excludes such a possibility $\dot{\nu} > \nu$ as $\dot{\nu}=1.2(1)$ [15]. Rather, our result supports the results of $\nu=0.44(2)$ ($\kappa=1$) with the Monte Carlo method [16] and $\nu=0.46(1)$ ($\kappa=1$) with the low-temperature-series-expansion result [17]. (The latter is obtained from $\dot{\alpha}=0.62(3)$ ($\kappa=1$) [17] together with the hyperscaling relation $\dot{\alpha}=2-d\dot{\nu}$.) Note that our preliminary survey in the preceding section also indicates a signature of $\dot{\nu} < \nu$.

Second, postulating the value $\dot{\nu} \approx 0.45$ close to the aforementioned existing values, we obtain an estimate for the

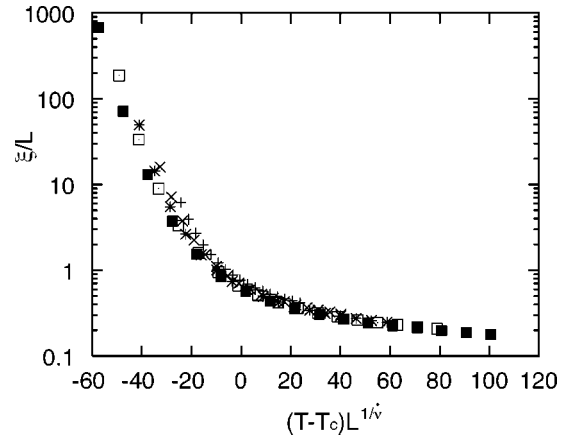


FIG. 6. Multicritical (crossover) scaling plot (14), $(T-T_c)L^{1/\dot{\nu}} - \xi/L$, for $\kappa=2$ and $\Delta L^{\phi/\dot{\nu}}=2$ is shown. Here, we set $\dot{\nu}=0.4$ and $\phi=0.6$, for which we found the best data collapse. The symbols $+$, \times , $*$, $*$, \square , and \blacksquare denote the system sizes of $N=5, 7, 9, 11$, and 13 , respectively.

crossover exponent $\phi \approx 0.43$. The present result contradicts the result $\phi=1.1(1)$ [19] determined with the cluster-variation method. In the succeeding section, we will provide further support to $\phi \approx 0.43$, performing the multicritical scaling analysis based on the relation (13).

C. Multicritical scaling analysis

In the above, we obtained an estimate for the crossover exponent $\phi \approx 0.43$ from the power-law singularity of the amplitude N^+ , accepting the value $\dot{\nu} \approx 0.45$ advocated by Refs. [16,17]. In this section, we provide further support to these exponents. We carry out a multicritical (crossover) scaling analysis based on Eq. (13). For finite size L , the scaling-hypothesis formula should be extended to

$$\xi = L\tilde{X}((T-T_c)L^{1/\dot{\nu}}, \Delta L^{\phi/\dot{\nu}}). \quad (14)$$

Based on this formula, in Fig. 6 we present the scaled data, $(T-T_c)L^{1/\dot{\nu}} - \xi/L$, with fixed $\Delta L^{\phi/\dot{\nu}}=2$ and $\kappa=2$. Here, we set the exponents $\dot{\nu}=0.4$ and $\phi=0.6$ for which we found the best data collapse. Surveying the parameter space beside this condition, we obtained the critical exponents as $\dot{\nu}=0.45(15)$ and $\phi=0.6(2)$. These estimates agree with the analysis in the preceding section.

We stress that the use of ξ greatly simplifies the scaling analyses, because ξ has a *fixed* scaling dimension, namely, $[\text{length}]^1$. For instance, as for other quantities such as the susceptibility, we need to determine the exponent $\dot{\gamma}$ in addition to $\dot{\nu}$. In this sense, the present approach via the transfer matrix is advantageous over other approaches.

IV. SUMMARY AND DISCUSSIONS

We investigated the (multi-) criticality of the gonihedric model (1) with the extended parameter space (2). The model is notorious for its slow relaxation to the thermal equilibrium (glassy behavior), which deteriorates the efficiency of the Monte Carlo sampling [22]. Aiming to surmount the diffi-

culty, we employed the transfer-matrix method. We implemented Novotny's idea [31–33], extending it so as to incorporate the plaquette-type interactions (Sec. II). The present approach enables us to treat an arbitrary number of spins per one transfer-matrix slice, admitting systematic finite-size-scaling analyses; see Fig. 4 for instance.

The transfer-matrix calculation has an advantage in that it yields the correlation length immediately. Because the correlation length has a known (fixed) scaling dimension, the subsequent scaling analyses are simplified significantly. Moreover, with the correlation length, we are able to calculate the Roomany-Wyld approximate β function $\beta_N^{RW}(T)$ (10). With the use of $\beta_N^{RW}(T)$, we surveyed the critical branch of the phase diagram (Fig. 3). Thereby, we observed that the criticality is maintained to be the three-dimensional-Ising universality class all along the phase boundary. On closer inspection, we found an indication of a crossover critical phenomenon such that the slope of $\beta_{13}^{RW}(T)$ in the off-critical regime, typically, $T - T_c > 3$ ($j = -0.05$), acquires a notable enhancement. This fact indicates that a multicriticality with smaller $\dot{\nu}$ emerges as $j \rightarrow -0.25$. This observation supports the claim [19] that the nonstandard criticality reported so far [15–20] could be attributed to the end-point criticality specific to $j = -0.25$.

Aiming to clarify the nature of this multicriticality, we analyzed the end-point singularity of the amplitude of the correlation length N^+ (12). As shown in Fig. 5, the amplitude exhibits a clear power-law singularity, from which we obtained an estimate for the singularity exponent $(-\dot{\nu} + \nu)/\phi = 0.415(20)$. This result supports the above-mentioned observation that an inequality $\dot{\nu} < \nu$ should hold, and in other words, it excludes such a possibility of $\dot{\nu} > \nu$ advocated in

Ref. [15]. Rather, our result supports the Monte Carlo simulation result $\dot{\nu} = 0.44(2)$ ($\kappa = 1$) [16] and the low-temperature-series-expansion result $\dot{\nu} = 0.46(1)$ ($\kappa = 1$) [17]. Postulating $\dot{\nu} \approx 0.45$, we arrive at an estimate for the crossover exponent $\phi \approx 0.43$. This exponent is to be compared with the result $\phi = 1.1(1)$ determined with the cluster-variation method [19]. The discrepancy between the result [19] and ours seems to be rather conspicuous.

We then carried out the multicritical scaling analysis (14) in order to provide further support to our estimate $\phi \approx 0.43$ based on $\dot{\nu} \approx 0.45$. We found that a good data collapse is attained for $\dot{\nu} = 0.4$ and $\phi = 0.6$ under $\kappa = 2$ and $\Delta L^{\phi/\dot{\nu}} = 2$ (Fig. 6). Surveying the parameter space, we obtained the estimates $\phi = 0.6(2)$ and $\dot{\nu} = 0.45(15)$. These exponents agree with the above-mentioned analysis via the critical amplitude N^+ .

As a consequence, we confirm that the whole analyses managed in this paper lead to a self-consistent conclusion. Regarding the discrepancy on ϕ , we suspect that the value $\phi = 1.1(1)$ [19] might be rather inconceivable. Nevertheless, in order to fix the multicriticality more definitely, further elaborate investigations would be required. As a matter of fact, a possible slight deviation of the multicritical point from $j = -0.25$ was ignored throughout the present work as in Ref. [19]. Justification of such a treatment might be desirable. In any case, the present approach, which is completely free from the slow-relaxation problem, would provide a promising candidate for a first-principles-simulation scheme in future research.

ACKNOWLEDGMENTS

This work was supported by Grant-in-Aid for Young Scientists (No. 15740238) from Monbu-kagakusho, Japan.

-
- [1] *Statistical Mechanics of Membranes and Surfaces, Volume 5 of the Jerusalem Winter School for Theoretical Physics*, edited by D. Nelson, T. Piran and S. Weinberg (World Scientific, Singapore, 1989).
 - [2] *Fluctuating Geometries in Statistical Mechanics and Field Theory*, edited by P. Ginsparg, F. David, and J. Zinn-Justin (Elsevier Science, The Netherlands, 1996).
 - [3] D. Horn and E. Katznelson, Phys. Lett. **121B**, 349 (1983).
 - [4] A. Maritan and A. Stella, Phys. Rev. Lett. **53**, 123 (1984).
 - [5] M. Karowski and H. J. Thun, Phys. Rev. Lett. **54**, 2556 (1985).
 - [6] M. Karowski, J. Phys. A **19**, 3375 (1986).
 - [7] G. K. Savvidy and F. J. Wegner, Nucl. Phys. B **413**, 605 (1994).
 - [8] G. K. Savvidy and K. G. Savvidy, Phys. Lett. B **324**, 72 (1994).
 - [9] G. K. Savvidy and K. G. Savvidy, Phys. Lett. B **337**, 333 (1994).
 - [10] G. K. Savvidy, K. G. Savvidy, and P. G. Savvidy, Phys. Lett. A **221**, 233 (1996).
 - [11] A. Cappi, P. Colangelo, G. Gonnella, and A. Maritan, Nucl. Phys. B **370**, 659 (1993).
 - [12] R. V. Ambartzumian, G. S. Sukiasian, G. K. Savvidy, and K. G. Savvidy, Phys. Lett. B **275**, 99 (1992).
 - [13] G. Koutsoumbas and G. K. Savvidy, Mod. Phys. Lett. A **17**, 751 (2002).
 - [14] D. Espriu, M. Baig, D. A. Johnston, and R. P. K. C. Malmini, J. Phys. A **30**, 405 (1997).
 - [15] D. A. Johnston and R. P. K. C. Malmini, Phys. Lett. B **378**, 87 (1996).
 - [16] M. Baig, D. Espriu, D. A. Johnston, and R. P. K. C. Malmini, J. Phys. A **30**, 7695 (1997).
 - [17] R. Pietig and F. J. Wegner, Nucl. Phys. B **525**, 549 (1998).
 - [18] E. N. M. Cirillo, G. Gonnella, D. Johnston, and A. Pelizzola, Phys. Lett. A **226**, 59 (1997).
 - [19] E. N. M. Cirillo, G. Gonnella, and A. Pelizzola, Phys. Rev. E **55**, R17 (1997).
 - [20] E. N. M. Cirillo, G. Gonnella, and A. Pelizzola, Nucl. Phys. B **63**, 622 (1998).
 - [21] E. N. M. Cirillo, G. Gonnella, M. Troccoli, and A. Maritan, J. Stat. Phys. **94**, 67 (1999).
 - [22] R. K. Hellmann, A. M. Ferrenberg, D. P. Landau, and R. W. Gerling, *Computer Simulation Studies in Condensed-Matter Physics IV*, edited by D. P. Landau, K. K. Mon, and H.-B. Schüttler (Springer-Verlag, Berlin, 1993).
 - [23] J. D. Shore and J. P. Sethna, Phys. Rev. B **43**, 3782 (1991).

- [24] M. R. Swift, H. Bokil, R. D. M. Travasso, and A. J. Bray, *Phys. Rev. B* **62**, 11494 (2000).
- [25] A. Lipowski, *J. Phys. A* **30**, 7365 (1997).
- [26] A. Lipowski and D. Johnston, *J. Phys. A* **33**, 4451 (2000).
- [27] A. Lipowski and D. Johnston, *Phys. Rev. E* **61**, 6375 (2000).
- [28] A. Lipowski, D. Johnston, and D. Espriu, *Phys. Rev. E* **62**, 3404 (2000).
- [29] E. K. Riedel and F. Wegner, *Z. Phys.* **225**, 195 (1969).
- [30] P. Pfeuty, D. Jasnow, and M. E. Fisher, *Phys. Rev. B* **10**, 2088 (1974).
- [31] M. A. Novotny, *J. Appl. Phys.* **67**, 5448 (1990).
- [32] M. A. Novotny, *Phys. Rev. B* **46**, 2939 (1992).
- [33] M. A. Novotny, *Phys. Rev. Lett.* **70**, 109 (1993).
- [34] M. A. Novotny, *Computer Simulation Studies in Condensed Matter Physics III*, edited by D. P. Landau, K. K. Mon, and H.-B. Schüttler (Springer-Verlag, Berlin, 1991).
- [35] H. H. Roomany and H. W. Wyld, *Phys. Rev. D* **21**, 3341 (1980).
- [36] A. M. Ferrenberg and D. P. Landau, *Phys. Rev. B* **44**, 5081 (1991).